

## A Theoretical Study of the Chorismate Synthase Reaction

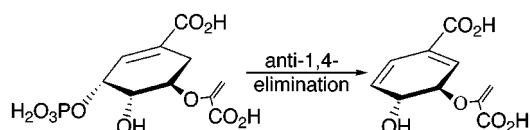
Olga Dmitrenko,<sup>†</sup> Harold B. Wood, Jr.,<sup>‡</sup> Robert D. Bach,<sup>\*,†</sup> and Bruce Ganem<sup>\*,‡</sup>

Department of Chemistry and Chemical Biology, Brown Laboratory, University of Delaware, Newark, Delaware 19716, and Department of Chemistry and Chemical Biology, Baker Laboratory, Cornell University, Ithaca, New York 14853-1301

bg18@cornell.edu

Received September 21, 2001

## ABSTRACT

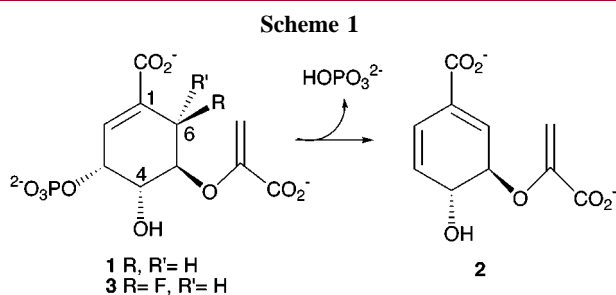


Density functional calculations (B3LYP/6-31+G(d,p)) were carried out to investigate the mechanism of the *anti*-1,4-elimination of phosphate from 5-enolpyruvylshikimate-3-phosphate **1** that is catalyzed by chorismate synthase. Of particular interest was the functional role of the reduced flavin cofactor.

The shikimic acid biosynthetic pathway generates a diverse array of aromatic amino acids and other metabolites in bacteria, fungi, and higher plants.<sup>1</sup> Chorismate synthase, the seventh enzyme of the main pathway, catalyzes the *anti*-1,4-elimination of phosphate from 5-enolpyruvylshikimate-3-phosphate **1** (EPSP) to generate chorismic acid **2** (Scheme 1), an important branch point metabolite. While several

The mechanism of the chorismate synthase reaction has attracted much interest.<sup>3–5</sup> Of the various possibilities, a concerted E2 or nonconcerted E1cb elimination involving deprotonation at C6 would likely require a strong base. An E1 mechanism is disfavored because phosphate monoesters, which are anionic at physiological pH, make comparatively poor leaving groups<sup>6</sup> and because phosphorolysis would be retarded by the electron-withdrawing C $\alpha$ -inductive effect at C4 in **1**.<sup>7</sup> Moreover, all known chorismate synthases require a reduced flavin (FMNH<sub>2</sub>) for catalysis, and none of the mechanisms yet propounded adequately explains the role of the flavin.

Recent studies favor a radical mechanism, based on the observance of (i) a transient flavin intermediate ( $\lambda_{\text{max}} = 400$  nm) detected in single turnover experiments,<sup>8</sup> (ii) a stabilized



microbial and plant chorismate synthases have been characterized, most studies to date have employed either the *E. coli* or *N. crassa* enzyme.<sup>2</sup>

(1) (a) Haslam, E. *Shikimic Acid Metabolism and Metabolites*; John Wiley & Sons: New York, 1993; (b) Bentley, R. *Crit. Rev. Biochem. Mol. Biol.* **1990**, *25*, 307–384.

(2) For a recent review, see: Macheroux, P.; Schmid, J.; Amrhein, N.; Schaller, A. *Planta* **1999**, *207*, 325–334.

(3) Walsh, C. T.; Liu, J.; Rusnak, F.; Sakaitani, M. *Chem. Rev.* **1990**, *90*, 1105–1129.

(4) Bornemann, S.; Lowe, D. J.; Thorneley, R. N. F. *Biochem. Soc. Trans.* **1996**, *24*, 84–88.

(5) Bornemann, S.; Lowe, D. J.; Thorneley, R. N. F. *Biochemistry* **1996**, *35*, 9907–9916.

(6) Westheimer, F. H. *Science* **1987**, *235*, 1173–1178.

(7) Lloyd, D. J.; Parker, A. J. *Tetrahedron Lett.* **1970**, 5029–5032.

(8) Ramjee, M. N.; Coggins, J. R.; Hawkes, T. R.; Lowe, D. J.; Thorneley, R. N. F. *J. Am. Chem. Soc.* **1991**, *113*, 8566.

<sup>†</sup> University of Delaware.

<sup>‡</sup> Cornell University.

enzyme-bound flavin semiquinone radical formed in the presence of the inhibitor 6*R*-6-fluoro-EPSP **3**,<sup>9</sup> and (iii) a significant secondary  $\beta$ -deuterium isotope effect using [4-<sup>2</sup>H]-EPSP.<sup>10</sup> Here we describe density functional calculations for the chorismate synthase reaction that shed light on the various mechanistic proposals and on the functional role of the reduced flavin.

Optimized geometries (B3LYP/6-31+G(d,p)) were calculated for *cis*-3,4-dihydroxycyclohexene-1-carboxylic acid-3-phosphate (DHCCP, Figure 1a) and the corresponding

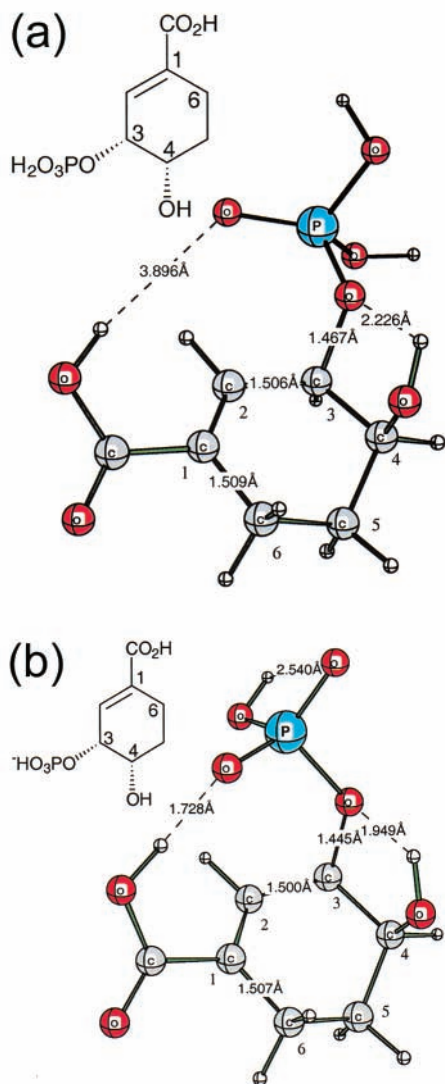


**Figure 1.** (a) Optimized geometry for neutral DHCCP. (b) Optimized geometry for DHCCP phosphate anion.

phosphate monoanion (Figure 1b) as a model<sup>11</sup> for **1** using the Becke three-parameter hybrid functional combined with

(9) Ramjee, M. N.; Balasubramanian, S.; Abell, C.; Coggins, J. R.; Davies, J. M.; Hawkes, T. R.; Lowe, D. J.; Thorneley, R. N. F. *J. Am. Chem. Soc.* **1992**, *114*, 3151–3153.

(10) Bornemann, S.; Theoclitou, M.-E.; Brune, M.; Webb, M. R.; Thorneley, R. N. F.; Abell, C. *Bioorg. Chem.* **2000**, *28*, 191–204.

the Lee, Yang, and Parr (LYP) correlation functional, denoted B3LYP.<sup>12,13</sup> In both calculations, the C3-phosphate group in DHCCP forms a strong hydrogen bond with the *syn*-C4-hydroxyl group, which would be expected to promote phosphorolysis. Additional H-bonding between the phosphate and the C1-carboxyl group gives rise to a bidentate interaction (ca. 6–8 kcal/mol each)<sup>14</sup> that also favors phosphorolysis. The interactions are more pronounced in the phosphate anion (Figure 1b), which forms a stronger, closer H-bond between the phosphate oxygen and the carboxylic acid group, along with a somewhat shorter C3–O bond length. Counterparts to these gas-phase interactions may be provided by chorismate synthase active site residues.

To investigate the E1cb process, deprotonation at C6 was modeled using DHCCP, and the structure of the resulting anion was optimized (Figure 2). The relatively low calculated

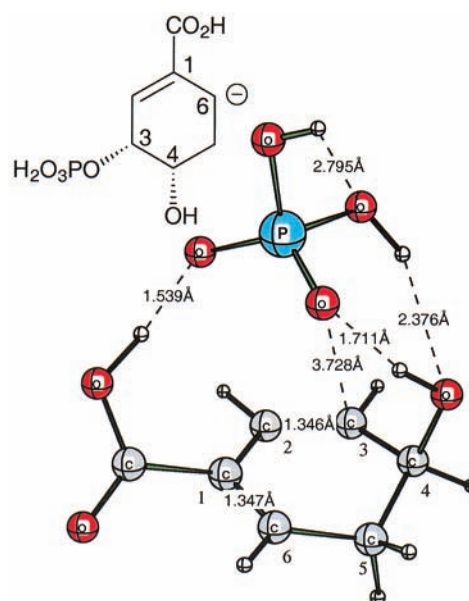


**Figure 2.** Optimized geometry for DHCCP anion.

proton affinity<sup>15</sup> (PA) of the corresponding anion (307.2 kcal/mol) is lower than that of H<sub>2</sub>PO<sub>4</sub><sup>-</sup> (330.8 kcal/mol) and is comparable to that of the phosphate monoanion (Figure 1b, 313.8 kcal/mol), indicating that the C6 hydrogen is unusually acidic and may require only a weak base for deprotonation.

(11) DHCCP lacks the C5-enolpyruvate side chain of EPSP, which is *anti* to both the phosphate and hydroxyl groups in **1** and would not be expected to exert any stabilizing H-bonding effects. Moreover, the absence of the ether side chain should result in only minor conformational effects on the carbocyclic ring.

(12) (a) Becke, A. D. *Phys. Rev. A* **1988**, *37*, 785. (b) Lee, C.; Yang, W.; Parr, R. G. *Phys. Rev.* **1988**, *B41*, 785. (c) Becke, A. D. *J. Chem. Phys.* **1993**, *98*, 5648. (d) Stevens, P. J.; Devlin, F. J.; Chabrowski, C. F.; Frisch, M. J. *J. Phys. Chem.* **1994**, *80*, 11623.

(13) All calculations used the Gaussian 98 program: Frisch, M. J. et al. *Gaussian 98*; Gaussian, Inc.: Pittsburgh, PA, 1998.

(14) Bach, R. D.; Dmitrenko, O.; Glukhovtsev, M. N. *J. Am. Chem. Soc.* **2001**, *123*, 7134–7145.

(15) Calculated PA values were based on B3LYP/6-31+G(d,p) total energies and are typically within 1–2% of experimental values.

Consistent with that finding, the enzyme-catalyzed elimination of (6*R*)-[6-<sup>2</sup>H]-EPSP displayed a small kinetic isotope effect of ~1.13, which has since been attributed to a secondary effect at C6 on C3–O bond breakage.<sup>2</sup>

Surprisingly, the C3–O bond spontaneously cleaves during optimization of the C6-anion of DHCCP (C–O separation = 3.73 Å, Figure 2). Consistent with this observation the delocalized “carbanion” (Figure 2) is 6.7 kcal/mol lower in energy than its isomeric phosphate anion (Figure 1b) as a consequence of several anionic hydrogen bonds. Moreover, the charge distribution (calculated by Natural Bond Orbital Analysis<sup>13</sup>) in the fully optimized anion indicates loss of a strongly H-bonded phosphate group carrying 85% of the negative charge, as well as alkene-like C1–C6 and C2–C3 bond lengths resembling the incipient diene **2**. The absence of a measurable activation barrier is unusual for an E1cb 1,4-elimination, where the breaking C–H bond is unactivated.

All radical mechanisms proposed for the conversion of **1** to **2** begin with one-electron transfer from FMNH<sup>–</sup> to EPSP, followed by loss of phosphate to form an allylically stabilized radical intermediate.<sup>2</sup> To probe that process, the structure of the first-formed EPSP radical anion was modeled using DHCCP and optimized using the UB3LYP/6-31+ G(d,p) method (Figure 3). The “plus” basis better describes the

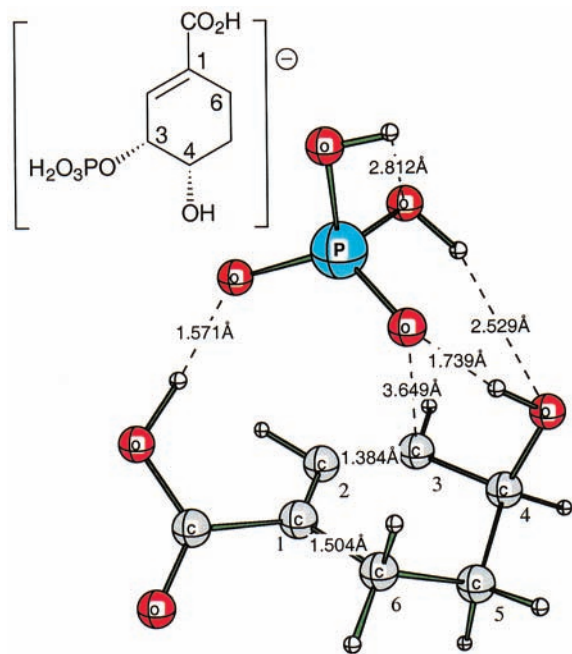


**Figure 3.** Optimized geometry for DHCCP radical anion.

oxygen lone pairs of the anion, and the polarization function on all hydrogen atoms more accurately treats the hydrogen bonds. Interestingly, the energy-minimized structure of the DHCCP radical anion undergoes C3–O bond rupture to the allylic radical and phosphate anion (C3–O bond distance 3.65 Å). As in the C6-anion, the departing phosphate is also

stabilized by numerous H-bonding interactions with both the C1 carboxylic acid and the C4 hydroxyl group, thereby reducing the negative charge on the departing phosphate ( $Q = -0.43 e$ ) and lowering the C–O dissociation barrier.

Of particular interest in the radical mechanism is the structure of the transient flavin intermediate. Formed before the substrate is consumed and decaying late in the catalytic cycle, the intermediate has been attributed to a charge-transfer complex, proton-transfer event, or protein conformational change before either C3–O or C6–H bond cleavage.<sup>5</sup> To shed light on this question, the energy minimum of the supermolecule formed between DHCCP and FMNH<sup>–</sup> was computed.

The structure of a partially optimized reactant complex at B3LYP/6-31G(d) (Figure 4)<sup>16</sup> indicates a sandwich-like

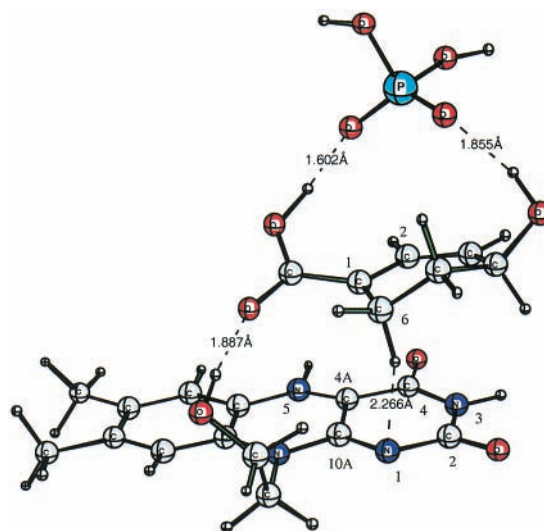


**Figure 4.** Partially optimized DHCCP–FMNH<sup>–</sup> complex (B3LYP/6-31G(d)).

structure in which the carbocyclic ring of DHCCP is lodged between the flavin and the departing, heavily complexed phosphate group. The complex is stabilized by favorable hydrogen bonding between the N10-hydroxyethyl group of the flavin and the C1-carboxyl group of DHCCP. An additional bonding interaction is evident between the breaking C6–H bond and N1 of the deprotonated flavin, which can project one electron pair to serve as the base in the *anti*-elimination leading to chorismate. The distances between N1 of the flavin and C6 in DHCCP as well as between C4 in the flavin and C2 in DHCCP were both fixed to 3.25 Å.

(16) The 2'OH of the ribityl side chain of FMNH<sup>–</sup> was modeled as a β-hydroxyethyl group. The geometry was optimized initially at B3LYP/3-21G\*\* until the forces but not displacements were fully converged. The distances between N1 of the FMNH<sup>–</sup> and C6 in DHCCP as well as between C4 in the flavin and C2 in DHCCP were both fixed to 3.25 Å, and optimization was continued at B3LYP/6-31G(d) (Figure 4) until the forces again converged. Further optimization at this level of theory resulted in loss of the sandwich-like structure and formation of a covalent bond between C4A of the flavin and C1 of DHCCP. This competition between H-bonding and covalent bonding might be resolved using a larger basis set, which is not currently practical for a system of this size.

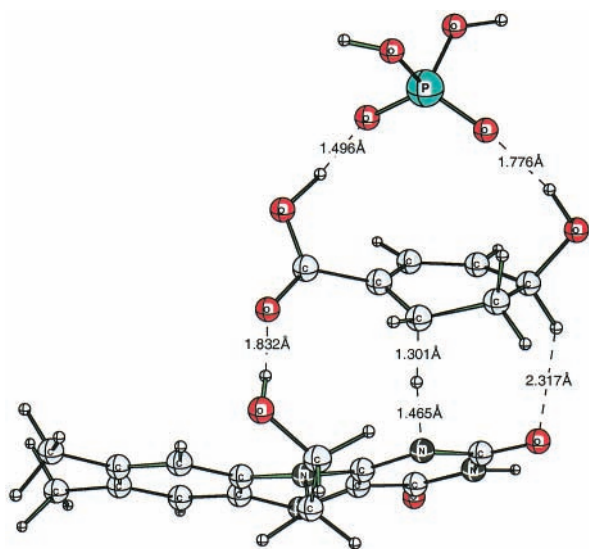


**Figure 5.** Fully optimized DHCCP-FMNH<sup>-</sup> transition structure for C6 deprotonation (B3LYP/6-31G(d)).

The calculated charge distribution in the minimized superstructure is also mechanistically illuminating. Nearly 75% of the net anionic charge resides on the substrate (almost equally distributed between the leaving phosphate group and the remainder of DHCCP) with about 25% on the flavin, which would be consistent with an initial, transient, EPSP/FMNH<sup>-</sup> charge-transfer complex (reported  $\lambda_{\text{max}} = 400$  nm) leading to charge transfer-induced C–O bond dissociation and concomitant deprotonation at C6. Partial electron transfer from the flavin would explain why no intermediate flavin semiquinone has been detected spectroscopically in enzymatic reactions with **1**.

The transition structure (Figure 5) for deprotonation at C6 is an early TS (first-order saddle point)<sup>17</sup> for proton transfer to N1 and displays a short-strong hydrogen bond between the H<sub>2</sub>PO<sub>4</sub><sup>-</sup> anion and C1-carboxyl (2.47 Å O–O distance). In addition, the structure rationalizes results observed with inhibitor **3**, since the absence of a 6*R*-hydrogen makes concomitant electron transfer and deprotonation impossible,

thus leading irreversibly to the flavin semiquinone, which has been documented experimentally.

Besides being consistent with reported experimental findings, the calculations presented in Figures 1–5 lead to three nonobvious conclusions about the chorismate synthase reaction. First, significant chelation effects are evident in the substrate (Figure 1A), which likely accelerate the elimination reaction. Second, the transition state shows that partial electron transfer from the flavin to bound EPSP actually induces phosphorolysis (charge on the H<sub>2</sub>PO<sub>4</sub><sup>-</sup> fragment is  $-0.83$  e), while also stabilizing the incipient electron deficiency at C3 (Figure 4). Third, calculated PA values (Figure 2) indicate increasing acidity at C6 as the C3–O bond breaks, with concomitant transfer of the *anti*-hydrogen at C6 to N1 of the flavin (Figure 5).

Thus the flavin cofactor plays a pivotal role in phosphorolysis, charge stabilization, electron transfer, and deprotonation in the chorismate synthase reaction. The findings presented here may also shed light on the mechanism of isopentenyl pyrophosphate isomerase, another recently reported, redox-neutral flavin-dependent enzyme that likely involves some of the same cofactor functions.<sup>18</sup>

**Acknowledgment.** We thank the NIH (GM 24054, to B.G.) and NSF (CHE-9901661, to R.D.B.) for support, and the National Center for Supercomputing Applications, Urbana, IL and Lexington, KY for computer time.

**Supporting Information Available:** Total energies (au) of selected fully optimized neutral and anion compounds, as well as total energies, Cartesian coordinates, and NBO charge distributions for the structures shown in the figures. This material is available free of charge via the Internet at <http://pubs.acs.org>.

OL0167964

(17) B3LYP/3-21G(d,p) full optimization and a frequency calculation were performed initially. The visualization of imaginary frequency ( $\nu = -940$  cm<sup>-1</sup>) confirmed a TS for proton transfer. The TS was then fully optimized at B3LYP/6-31G(d) with a single point calculation at the B3LYP/6-31+G(d,p) level. The estimated classical activation barrier is about 7 kcal/mol at the B3LYP/3-21G(d,p) and 11 kcal/mol at the B3LYP/6-31+G(d,p)/B3LYP/6-31G(d) level.

(18) Kaneda, K.; Kuzuyama, T.; Takagi, M.; Hayakawa, Y.; Seto, H. *Proc. Natl. Acad. Sci. U.S.A.* **2001**, *98*, 932–937.